Model geometry and setup: We design a model with a 200 km wide mountain range similar to the width of the Western Alps or the Pyrenees (Fig. 1). The topography consists of a 3km high narrow plateau surrounded by constant slopes on each side of the plateau. The model is extended to 500 km on each side of the range axis to avoid spurious edge effect related to the boundary conditions. The mountain range is initially isostatically compensated by a crustal root. We compute a geotherm in agreement with the average 60 mW/m^2 heat flow for the region surrounding the Western Alps and the Pyrenees (Lucazeau and Vasseur, 1989) and an average heat production of 1.3$\mu W/m^3$ in the crust. Initial state stress is setup to hydrostatic with respect to the height of topographic surface.

Model rheology: The model accounts for the rheological properties of the lithosphere with pressure–temperature dependent constitutive laws. For both upper crust and mantle, we use an elastoplastic pressure-dependent law with a Drucker–Prager failure criterion (Leroy and Ortiz, 1989). The friction angle is set to 15° to be consistent with a high internal friction ($\mu = 0.6$) and a hydrostatic pore pressure for the upper crust (Chéry et al., 2001). At high *P–T*, a strain rate dependent "power law" rheology is used. The rheological change between the upper seismogenic crust and the lower viscous crust depends on the temperature gradient of the region. The resulting stress in the mantle depends on both the chosen rheology and the thermal state. We use a quartzite rheology (Koch et al. 1989) for the viscous crust and a dry-olivine rheology for the mantle (Karato and Jung, 2003). Flow law parameters are summarized in the Table DR1. Because the chosen quartzite rheology is associated to a dry rock, the brittle-ductile transition may occur at a deeper depth that would happen if a wet crustal rock rheology had been chosen. The use of a more mafic rheology for the lower crust could also deepen the brittle-ductile transition. The state of stress at depth in the crust is therefore difficult to assess in the lack of reliable information about rock rheology and thermal state. In the mantle, the dry-olivine rheology that we use is likely maximizing the deviatoric stress level below the crustal root. We tested that a weaker mantle rheology decreases the deviatoric stress in the mantle, therefore bringing the mountain stress state closer to an isostatic behavior. Thus, upper crustal extension is favored by such a rheological change. A similar behavior (i.e., larger extension) is also obtained using higher temperature for the mountain root. By contrast, a cold lithosphere results in a distributed flexure in response to erosion and minimizes horizontal motions. In summary, significant mountain extension is likely to occur only for a relatively hot lithosphere.

Table DR1 : Model flow law $\dot{\varepsilon} = \gamma_0 \sigma^n \exp\left(-\frac{E}{RT}\right)$ linking the strain-rate $\dot{\varepsilon}$ and the deviatoric stress σ.

Layer	Pre-exponential fluidity γ_0 ($Pa^{-n}s^{-1}$)	Power law exponent *n*	Activation energy *E* (kJ/mol)	Reference
crust	$6.0\ 10^{-24}$	2.72	134	Koch et al. (1989)
mantle	$7.0\ 10^{-14}$	3.0	510	Karato and Jung (2003)

Surface erosion: Many surface processes associated with climate, rock strength or vegetation contribute to erosion and sedimentation in mountain ranges. Over the last decades a constant effort has been made to develop erosion laws to account for the complexity of these surface processes (*e.g.* Whipple and Tucker, 1999; Lavé, 2005; Sklar and Dieterich, 2006; Willet, 2010). Unfortunately, the parameters needed into these laws, like rock erodibility, power law exponents or critical shear stress, are often badly constrained and empirically estimated for each specific study area. Here, because we do not investigate the dynamics of landscape evolution in details, we favor the use of three simple laws, which offer a first order description consistent with the simplicity and main scope of this paper.
The erosion rate of the topographic model surface is taken proportional to the slope (Beaumont, 2001) in most models:

$$\frac{\partial h}{\partial t} = K_1 \frac{\partial h}{\partial x},$$

where h is the elevation, t the time, x the distance along the study profile and K_1 a constant. We also run some experiments for constant and uniform erosion

$$\frac{\partial h}{\partial t} = K_2$$

and diffusion law (Steer et al., 2010).

$$\frac{\partial h}{\partial t} = K_3 \frac{\partial^2 h}{\partial x^2}$$

In order to compare the results of these three erosion laws we normalize the amount of erosion by adjusting the constants K_i to obtain similar average erosion rate defined as

$$\left.\frac{\partial h}{\partial t}\right|_{average} = \frac{1}{x_{\max} - x_{\min}} \int_{x_{\min}}^{x_{\max}} \frac{\partial h}{\partial t} dx = \frac{K_1}{200} \int_{-100}^{100} \frac{\partial h}{\partial x} dx = \frac{K_2}{200} \int_{-100}^{100} dx = \frac{K_3}{200} \int_{-100}^{100} \frac{\partial^2 h}{\partial x^2} dx$$

with x_{max} - x_{min} is the width of the width of the initial topography. Figure A1 gives the distribution of erosion across the range for the three erosion laws used in this study after 0.5 Myr and for an average erosion rate of 0.75 mm/yr.

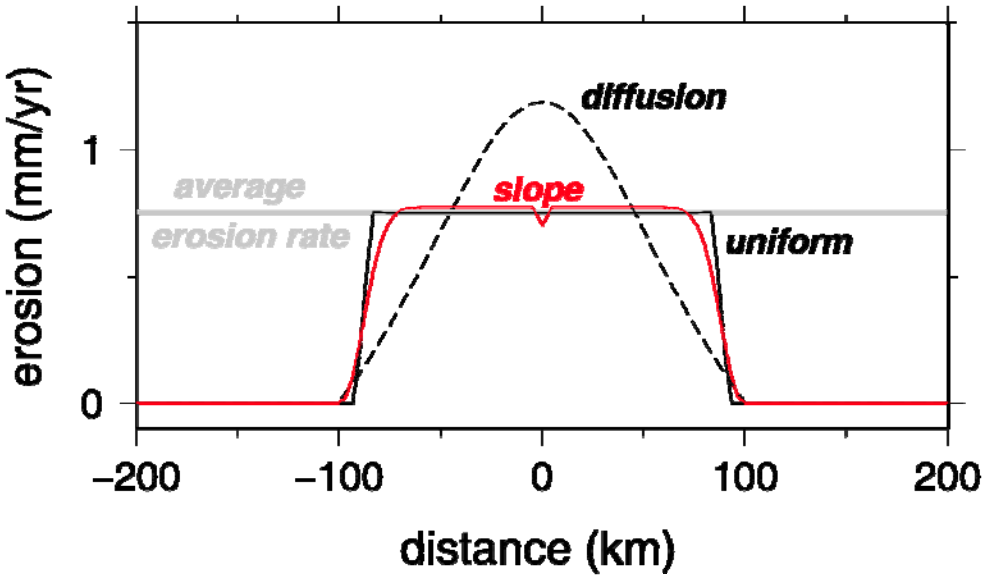

Figure DR1: Erosion rate across the range obtained after 0.5 Myr and for an average erosion rate of 0.75 mm/yr. Three erosion laws are considered: an erosion proportional to the slope (red line), a constant and uniform erosion (solid line) and a diffusion law (dashed line).

Beaumont, C., Jamieson, R. A., Nguyen, M. H. & Lee, B. , 2001, Himalayan tectonics explained by extrusion of a low-viscosity crustal channel coupled to focused surface denudation: Nature, v. 414, p. 738–742.

Chéry, J., Zoback, M.D., and Hassani, R., 2001, An integrated mechanical model of the San Andreas Fault in central and northern California: J. Geophys. Res., v. 106, p. 22051-22066.

Karato, S. I., Jung, H., 2003, Effects of Pressure on High-Temperature Dislocation Creep in Olivine Polycrystals, Philosophical Magazine, 83: 401–414.

Koch, P. S., J. M. Christie, A. Ord, and R. P. George Jr., 1989, Effect of water on the rheology of experimentally deformed quartzite, J. Geophys. Res., *94*(B10), 13,975–13,996, doi:10.1029/JB094iB10p13975.

Leroy, Y., and Ortiz, M., 1989, Finite element analysis of strain localization in frictional materials: Int. J. Numer. Anal. Methods Geomech., v. 13, p. 53-74.

Lavé, J., 2005, Analytic solution of the mean elevation of a watershed dominated by fluvial incision and hillslopes landsliding. Geophysical Research Letters, 32(11), L11403.

Lucazeau, F., and Vasseur, G., 1989, Heat flow density data from France and surrounding margins: Tectonophysics, v. 164, p. 251-258.

Sklar, L.S. and W.E. Dietrich, 2006. The role of sediment in controlling bedrock channel slope: Implications of the saltation-abrasion incision model, Geomorphology, Vol. 82, No. 1-2, p. 58-83, doi:10.1016/j.geomorph.2005.08.019.

Steer, P., Cattin, R., Lavé, J., and Godard, V., 2010, Surface Lagrangian Remeshing: a new tool for studying long-term evolution of continental lithosphere from a 2D numerical modeling: Computers and Geosciences, v. 27, p. 1067-1074.

Whipple, K.X, and Tucker, G.E., 1999, Dynamics of the stream-power river incision model: Implications for height limits of mountain ranges, landscape response timescales, and research needs, : J. Geophys. Res., v. 104, p. 17,661-17,674.